Magnetically controllable intra-Brillouin-zone band gaps in one-dimensional helicoidal magnetophotonic crystals

Fei Wang
Research and Development, Micron Technology, Inc., Boise, Idaho 83707-0006, USA

A. Lakhtakia
Department of Engineering Science and Mechanics, Nanoengineered Metamaterials Group, Pennsylvania State University, University Park, Pennsylvania 16802-6812, USA

(Received 1 March 2009; published 7 May 2009)

Interleaving magnetophotonic garnet layers with layers of a structurally chiral material (SCM) leads to a one-dimensional helicoidal magnetophotonic crystal, the interaction of whose overall period and the helicoidal period of the SCM layers leads to intra-Brillouin-zone photonic band gaps which depend on the structural handedness of the SCM layers and whose gap widths are magnetically controllable. Even as the overall period grows very large, one photonic band gap remains unaffected as it is due to the helicoidal period. Also, the gap widths can be magnetically decreased by turning up the magnitude of the externally impressed dc magnetic field.

DOI: 10.1103/PhysRevB.79.193102 PACS number(s): 42.70.Qs, 42.25.Bs, 78.20.Ls

I. INTRODUCTION

Light incident normally on a sufficiently thick periodic stack of two or more dissimilar materials can be highly reflected if the frequency of light lies in a Bragg zone. The center frequency and the bandwidth of a Bragg zone are dependent on the photonic properties of the materials and the thicknesses of the layers in the unit cell.[1] The periodic stack is a one-dimensional (1D) photonic crystal (PC) and the Bragg zone is a photonic band gap (PBG). The center frequency of a PBG is inversely proportional to the structural period of a 1D PC, which can operate as a Bragg filter.

The photonic properties of ferrimagnetic garnets are strongly influenced by an externally impressed magnetic field.[2] If at least one constituent material of a PC is a ferrimagnetic garnet, the center frequencies and the gap widths of the PBGs are magnetically tunable.[3–5] Other factors such as misalignment between the optic axes of two consecutive layers in the unit cell of a 1D magnetophotonic crystal (MPC) can either aid or impede magnetic tunability.[6]

Multiple structural periodicities are desirable for 1D MPCs to operate in multiple frequency bands, each band being magnetically tunable. One way to accomplish that is to interleave homogeneous layers of a ferrimagnetic garnet with layers of a structurally chiral material (SCM)—such as a chiral liquid crystal[7] or a chiral sculptured thin film[8]—which has a helicoidal morphology and is therefore periodically inhomogeneous by itself. Having thus proposed this 1D helicoidal magnetophotonic crystal (HMPC) with two periodicities, our task now is to examine how the overall periodicity of the HMPC and the periodicity of one of its two constituent materials (the SCM) interact to yield distinctive photonic-band-structure features.

II. THEORY

The thickness of the magnetophotonic garnet layer in the unit cell is denoted by d_m and that of the nonmagnetophotonic SCM layer by d_h. The overall period is thus $\Lambda = d_m + d_h$. The relative permittivity tensors of the two materials (superscripted $^{(m)}$ and $^{(h)}$, respectively) are as follows:

$$\underline{\underline{\epsilon}}^{(m)} = \begin{bmatrix} \bar{\epsilon}^{(m)} - \Delta^{(m)} & i\epsilon_g & 0 \\ -i\epsilon_g & \bar{\epsilon}^{(m)} + \Delta^{(m)} & 0 \\ 0 & 0 & \epsilon_{zz}^{(m)} \end{bmatrix}, \tag{1}$$

$$\underline{\underline{\epsilon}}^{(h)} = \underline{\underline{S}}\left(h\frac{\pi z}{\Omega}\right)\mathrm{Diag}[\bar{\epsilon}^{(h)} + \Delta^{(h)}, \bar{\epsilon}^{(h)} - \Delta^{(h)}, \bar{\epsilon}^{(h)} + \Delta^{(h)}]\underline{\underline{S}}^{-1}\left(h\frac{\pi z}{\Omega}\right). \tag{2}$$

Here ϵ_g indicates the optical gyrotropy of the garnet that manifests itself when an external dc magnetic field is applied parallel to the thickness direction (the z axis); the rotational tensor

$$\underline{\underline{S}}(\zeta) = \begin{bmatrix} \cos\zeta & -\sin\zeta & 0 \\ \sin\zeta & \cos\zeta & 0 \\ 0 & 0 & 1 \end{bmatrix}, \tag{3}$$

is needed to describe the helicoidal variation in the SCM morphology along the z axis; 2Ω is the helicoidal period but Ω is the dielectric period for light propagation along the z axis;[9] $h = \pm 1$ represents the structural handedness of the SCM layer and therefore of the HMPC; and $\bar{\epsilon}^{(m,h)}$, $\Delta^{(m,h)}$, and $\epsilon_{zz}^{(m)}$ represent the scalar permittivities when the external magnetic field is absent. We characterize the optical gyrotropy through the magnetophotonic angle $\alpha = \tan^{-1}[\epsilon_g/\Delta^{(m)}]$. For simplicity, the SCM is assumed to be locally uniaxial and both materials are assumed to be nondispersive, nondissipative, and nonmagnetic. The two materials can be dielectrically similar ($\bar{\epsilon}^{(m)} = \bar{\epsilon}^{(h)}$ and $\Delta^{(m)} = \Delta^{(h)}$) or not. An $\exp(-i\omega t)$ time dependence is implicit.

Suppose that the electromagnetic-field phasors are independent of x and y. Wave propagation inside the 1D HMPC

 ©2009 The American Physical Society

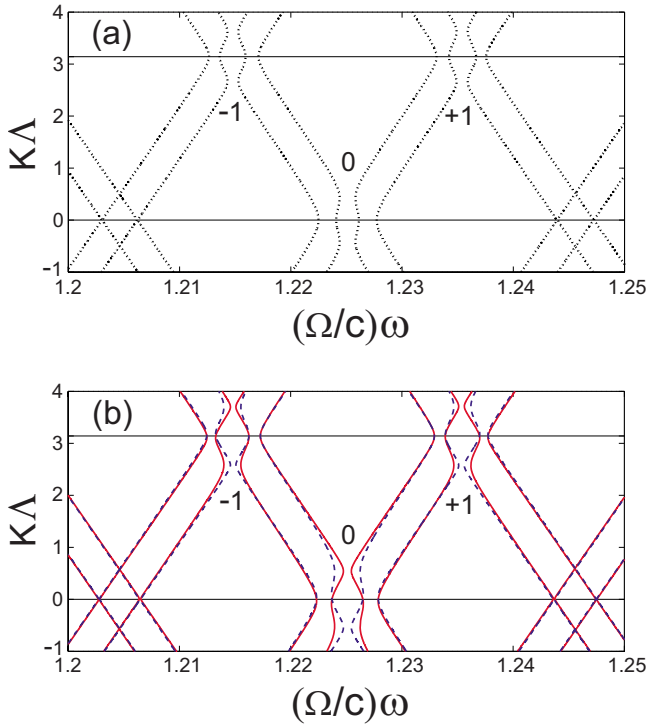

FIG. 1. (Color online) Brillouin diagrams for 1D HMPC with (a) $\alpha=0$ and (b) $\alpha=\pi/6$. The two materials in the unit cell are dielectrically similar: $\bar{\epsilon}^{(m)}=\bar{\epsilon}^{(h)}=6.576$ and $\Delta^{(m)}=\Delta^{(h)}=0.035$, which values are typical of bismuth iron garnet in the infrared regime (Ref. 11). Dimensions are: $d_m=d_h=0.5\Lambda=60\Omega$. The dotted lines in (a) are for the HMPC of either handedness, the solid lines in (b) are for the left-handed HMPC ($h=-1$), and the dashed lines in (b) are for the right-handed HMPC ($h=1$). Intra-Brillouin-zone PBGs in the diagrams are labeled by 0 and ±1.

can then be formulated using standard techniques.[5,10] The overall periodicity of the 1D HMPC permits invocation of the Floquet-Bloch theorem, whereby Bloch states emerge as solutions of the eigenvalue problem

$$\mathbf{D}^{(m)^{-1}}\mathbf{Y}^{(h)}\mathbf{W}^{(h)}\mathbf{Y}^{(h)^{-1}}\mathbf{D}^{(m)}\mathbf{P}^{(m)}\mathbf{A}_j^{(m)}=\exp(iK\Lambda)\mathbf{A}_j^{(m)}. \quad (4)$$

Here, K is the Bloch wave number; $\mathbf{A}_j^{(m)}$ is a column four vector containing eigenmodal amplitudes for the garnet layer in the jth unit cell; the 4×4 matrices $\mathbf{D}^{(m)}$ and $\mathbf{P}^{(m)}$ are explicitly expressed in Ref. 5; $\mathbf{W}^{(h)}$ is a transfer matrix for the SCM layer available in Ref. 10; and the auxiliary matrix $\mathbf{Y}^{(h)}$ is determined by enforcing the continuity of the tangential components of the electromagnetic field phasors across the interface between the two constituent layers of the unit cell. Solution of Eq. (4) yields the relationship between K and the angular frequency ω. Propagating Bloch states are indicated by real-valued K and evanescent Bloch states by complex-valued K; PBGs can thus be identified in Brillouin diagrams.

III. NUMERICAL RESULTS AND DISCUSSION

Figure 1 shows the Brillouin diagrams for a 1D HMPC made of dielectrically similar materials, when the external magnetic field is either absent ($\alpha=0$) or present ($\alpha=\pi/6$). Several PBGs are present inside the Brillouin zone near the zone boundaries $K\Lambda=0$ and π. The band profiles around these intra-Brillouin-zone PBGs are dependent on the structural handedness parameter h for $\alpha>0$ but not for $\alpha=0$; however, the gap widths are handedness-independent regardless of α.

For convenience, we classify the PBGs into groups $\mathcal{A}$ and $\mathcal{B}$ when they are in close proximity of the zone boundaries $K\Lambda=0$ and $K\Lambda=\pi$, respectively; furthermore, PBGs in group $\mathcal{A}$ are labeled $\{0,\pm2,\pm4,\ldots\}$, while those in group $\mathcal{B}$ are labeled $\{\pm1,\pm3,\pm5,\ldots\}$. In Fig. 1, group $\mathcal{A}$ is represented only by the PBG labeled 0, whereas group $\mathcal{B}$ is fully populated, which becomes evident when the horizontal axis is extended beyond the limits shown in the figure. PBGs not labeled 0 reflect the interaction of the overall period Λ with the electromagnetic field, being found when Ω is finite (HMPCs) and even in the limit $\Omega\to\infty$ (nonhelicoidal MPCs). In contrast, the PBG labeled 0 is located at $\omega=(\pi/\sqrt{\bar{\epsilon}^{(h)}})(c/\Omega)$, which is the center frequency of the Bragg regime of the SCM layer.[8,10] Thus, the PBG labeled 0 exists only for HMPCs (finite Ω) but not for nonhelicoidal MPCs ($\Omega\to\infty$).

In an isolated SCM layer with a sufficient number N_h of periods, a PBG is known to occur when a central phase defect is introduced in the form of a twist defect,[12,13] a spacer layer,[14] or some combination of twist defects and spacer layers.[8,14] Because of the phase interruption, a resonance occurs in the isolated SCM layer. The resonance is localized spatially at the defect site and spectrally at the center of the Bragg regime. This resonance can be excited by left- and right-circularly polarized light. When the handedness of the incident circularly polarized light is the same as the structural handedness of the isolated SCM layer, the resonance develops and vanishes as N_h is increased from a small value. When the two handednesses differ, the resonance develops and saturates as N_h is increased from a large value[12,13] because the localized energy density increases drastically with N_h until attaining a saturation level—this phenomenon is manifested in the Brillouin diagram as a PBG that blocks arbitrarily polarized light from propagating through the isolated SCM layer containing a central phase defect.

Given the existence of PBGs in isolated SCM layers with central phase defects and as the PBG labeled 0 does not exist when $d_m=0$ in the 1D HMPC, we conclude that this PBG is solely due to each magnetophotonic garnet layer acting as a phase defect inserted between two identical SCM layers with sufficiently large numbers of periods. Also, this PBG is, at best, weakly affected by the ratio $0.5\Lambda/\Omega$ of the overall period to the helicoidal period. This becomes clear from Fig. 2 which displays the center frequencies (ω_{bc}) and the gap widths ($\Delta\omega$) of the PBGs labeled 0 and ±1 in Fig. 1(b) as functions of Λ/Ω.

In contrast, the PBGs labeled ±1 in Fig. 1(b) exhibit notable dependences on the ratio Λ/Ω. For a fixed helicoidal period, the center frequencies and the gap widths of these two PBGs from group $\mathcal{B}$ appear to vary as $\sim\Lambda^{-1}$. This tendency is generally observed for PBGs in single-period nonhelicoidal PCs,[15] thereby affirming that the PBGs of group $\mathcal{B}$ are intimately connected to the overall periodicity of the 1D

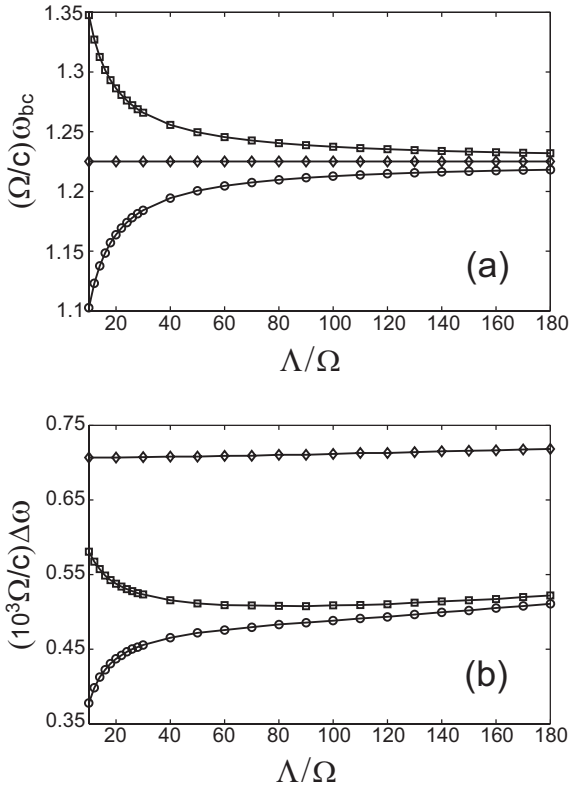

FIG. 2. The dependences of (a) the center frequencies ω_{bc} and (b) the gap widths $\Delta\omega$ of intra-Brillouin-zone PBGs on the ratio Λ/Ω. Lines with $\diamond$, $\square$, and $\bigcirc$ are for the PBGs labeled 0, +1, and −1, respectively, in Fig. 1(b).

HMPC. But the helicoidal periodicity also affects these PBGs significantly. For fixed Ω, as Λ increases, (i) their center frequencies approach the center frequency of the PBG labeled 0 and (ii) their gap widths remain finite. This is because the HMPC retains the helicoidal periodicity of the SCM layer even in the limit $\Lambda \to \infty$. Were this HMPC to be made nonhelicoidal by setting $h=0$ in Eq. (2), the center frequencies and gap widths of all PBGs would go to zero as $\Lambda \to \infty$.

The magnetic tunability of the PBGs of the 1D HMPC of Fig. 1 is illustrated in Fig. 3. PBGs in both groups $\mathcal{A}$ and $\mathcal{B}$ depend on α. The tunabilities of the gap widths of the higher-frequency PBGs (with labels $\in\{0,1,3,5,\ldots\}$) differ from those of the lower-frequency PBGs (with labels $\in\{-1,-3,-5,\ldots\}$). The gap widths of the higher-frequency PBGs decline linearly with increase in $\sin\alpha$. The gap widths of the lower-frequency PBGs first decrease to zero and then increase as $\sin\alpha$ increases. For each of the lower-frequency PBGs, we can designate a closure value α_c of α as follows: when $\alpha=\alpha_c$, the gap width vanishes and so does the PBG. The farther that a negatively labeled PBG is from the PBG labeled 0 on the ω axis, the lower is the value of the former's closure angle.

Figure 3 shows that the magnetic tunability of gap widths in HMPCs differs from that in nonhelicoidal MPCs in a significant manner. The gap widths in nonhelicoidal MPCs increase with α.[5,6] In contrast, the gap widths in HMPCs decrease as α increases for the higher-frequency PBGs and

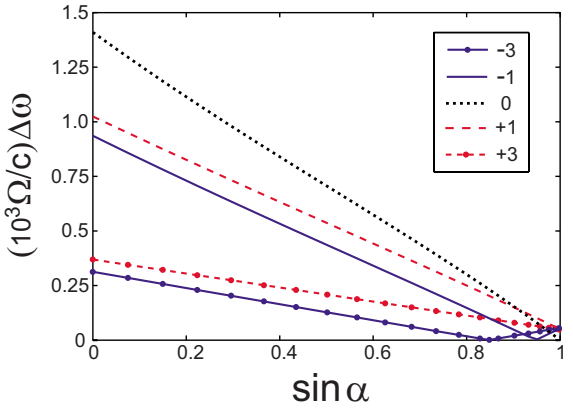

FIG. 3. (Color online) The dependences of the gap widths $\Delta\omega$ of intra-Brillouin-zone PBGs on α. All parameters are the same as for Fig. 1 except $\Lambda=20\Omega$.

prior to the closure angle α_c for the lower-frequency PBGs. The role of the helicoidal periodicity diminishes in the lower-frequency regime because the SCM layer of the HMPC tends to become effectively homogeneous as $(\omega/c)\Omega \to 0$. In other words, the optical role of helicoidal periodicity can be trumped by the post-α_c magnetically induced optical gyrotropy at sufficiently low frequencies.

Both groups $\mathcal{A}$ and $\mathcal{B}$ of PBGs are also exhibited by a 1D HMPC made of dielectrically dissimilar materials such that $\bar{\epsilon}^{(m)} \neq \bar{\epsilon}^{(h)}$ and/or $\Delta^{(m)} \neq \Delta^{(h)}$. As shown in Fig. 4, the ampli-

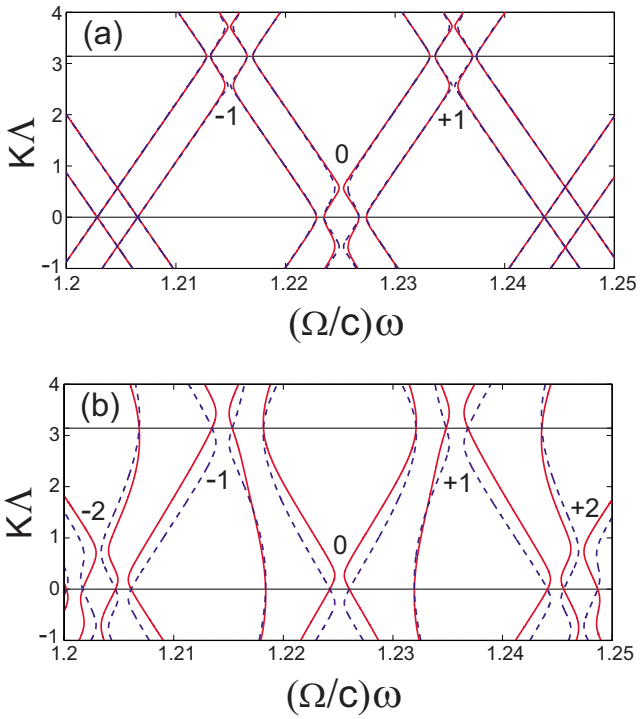

FIG. 4. (Color online) Brillouin diagrams for 1D HMPC made of dielectrically dissimilar materials such as (a) $\Delta^{(h)}=0.5\Delta^{(m)}$ and (b) $\Delta^{(h)}=5\Delta^{(m)}$. Other parameters are as follows: $\Delta^{(m)}=0.035$, $\bar{\epsilon}^{(m)}=\bar{\epsilon}^{(h)}=6.576$, $\alpha=\pi/6$, and $d_m=d_h=0.5\Lambda=60\Omega$. The solid lines are for the left-handed HMPC ($h=-1$) and the dashed lines are for the right-handed HMPC ($h=1$).

tudes of the uniaxial-anisotropy parameters $\Delta^{(m)}$ and $\Delta^{(h)}$ affect the center frequencies and the gap widths of PBGs. Increase in these parameters tend to amplify the gap widths, as may be seen by comparing the gap widths in Fig. 4(a) for lower $\Delta^{(h)}$ with those in Fig. 4(b) for higher $\Delta^{(h)}$. Furthermore, the density of PBGs on the ω axis increases as well, for which the two parts of Fig. 4 contain evidence. Finally, the effect of structural handedness gets amplified, as may be seen by comparing Figs. 1(b) and 4(b), both having been drawn for all constitutive and geometric parameters the same except for $\Delta^{(h)}$.

IV. CONCLUDING REMARKS

In this communication, we have delineated the characteristic features of intra-Brillouin-zone PBGs that are displayed by a 1D HMPC because the effects of its overall period Λ are significantly modified by the helicoidal period 2Ω of the SCM layer contained in its unit cell. One of the PBGs (labeled 0) occurs entirely due to a saturated wave resonance that occurs because each magnetophotonic garnet layer acts as a phase defect inserted between two identical SCM layers with sufficiently large numbers of periods. The helicoidal period is responsible for other qualitative differences with respect to nonhelicoidal MPCs. For example, the center frequencies of all PBGs approach a nondiminishing value even as $\Lambda \to \infty$ and the gap widths of the PBGs can be magnetically decreased by increasing the magnetophotonic angle by turning up the magnitude of an externally impressed dc magnetic field. These magnetically controllable PBGs are also affected by the structural handedness of the HMPC.

One-dimensional HMPCs can be conceived to display even more remarkable photonic-band-structure features. For instance, crystalline misalignment may be introduced by twisting all the magnetophotonic garnet layers by a certain angle about the z axis,[6] which would introduce new features even when the magnetophotonic garnet and the SCM are dielectrically similar. Another possibility is to use ferroelectric crystals for the magnetophotonic layers, which would introduce additional control by an externally impressed dc electric field. Yet another possibility is that the magnetophotonic layers also have a helicoidal morphology; then the additional helicoidal periodicity would introduce new features. All these potential new features about the 1D HMPC are worthy of being explored in the future.

[1] H. A. Macleod, *Thin-Film Optical Filters*, 3rd ed. (IOP, Bristol, 2001).
[2] J. I. Gersten and F. W. Smith, *The Physics and Chemistry of Materials* (Wiley, New York, 2001).
[3] I. L. Lyubchanskii, N. N. Dadoenkova, M. I. Lyubchanskii, E. A. Shapovalov, and Th. Rasing, J. Phys. D **36**, R277 (2003).
[4] S. Kahl and A. Grishin, Appl. Phys. Lett. **84**, 1438 (2004).
[5] M. Levy and A. A. Jalali, J. Opt. Soc. Am. B **24**, 1603 (2007).
[6] F. Wang and A. Lakhtakia, Appl. Phys. Lett. **92**, 011115 (2008).
[7] S. Chandrasekhar, *Liquid Crystals*, 2nd ed. (Cambridge University Press, Cambridge, 1992).
[8] I. J. Hodgkinson, Q. Wu, L. De Silva, M. Arnold, M. W. McCall, and A. Lakhtakia, Phys. Rev. Lett. **91**, 223903 (2003).
[9] A. Lakhtakia and V. C. Venugopal, AEU—Intl. Electron. Commun. **53**, 287 (1999).
[10] F. Wang and A. Lakhtakia, Opt. Express **13**, 7319 (2005).
[11] X. Huang, R. Li, H. Yang, and M. Levy, J. Magn. Magn. Mater. **300**, 112 (2006).
[12] V. I. Kopp and A. Z. Genack, Phys. Rev. Lett. **89**, 033901 (2002).
[13] F. Wang and A. Lakhtakia, Proc. R. Soc. London, Ser. A **461**, 2985 (2005).
[14] A. Lakhtakia, Opt. Commun. **275**, 283 (2007).
[15] J. Li, L. Zhou, C. T. Chan, and P. Sheng, Phys. Rev. Lett. **90**, 083901 (2003).